Derepression of hTERT gene expression promotes escape from oncogene-induced cellular senescence

Priyanka Patel, Anitha Suram, Neena Mirani, Oliver Bischof, Utz Herbig

Derepression of *hTERT* gene expression promotes escape from oncogene-induced cellular senescence

Priyanka L. Patel[a], Anitha Suram[a], Neena Mirani[b], Oliver Bischof[c,d], and Utz Herbig[a,e,1]

[a]New Jersey Medical School-Cancer Center, Rutgers Biomedical and Health Sciences, Newark, NJ 07103; [b]Department of Pathology and Laboratory Medicine, New Jersey Medical School, Rutgers Biomedical and Health Sciences, Newark, NJ 07103; [c]Nuclear Organization and Oncogenesis Unit, Department of Cell Biology and Infection, Institut Pasteur, 75015 Paris, France; [d]INSERM U993, F-75015 Paris, France; and [e]Department of Microbiology, Biochemistry, and Molecular Genetics, Rutgers Biomedical and Health Sciences, Rutgers University, Newark, NJ 07103

Edited by Victoria Lundblad, Salk Institute for Biological Studies, La Jolla, CA, and approved June 27, 2016 (received for review February 11, 2016)

Oncogene-induced senescence (OIS) is a critical tumor-suppressing mechanism that restrains cancer progression at premalignant stages, in part by causing telomere dysfunction. Currently it is unknown whether this proliferative arrest presents a stable and therefore irreversible barrier to cancer progression. Here we demonstrate that cells frequently escape OIS induced by oncogenic H-Ras and B-Raf, after a prolonged period in the senescence arrested state. Cells that had escaped senescence displayed high oncogene expression levels, retained functional DNA damage responses, and acquired chromatin changes that promoted c-Myc–dependent expression of the human telomerase reverse transcriptase gene (*hTERT*). Telomerase was able to resolve existing telomeric DNA damage response foci and suppressed formation of new ones that were generated as a consequence of DNA replication stress and oncogenic signals. Inhibition of MAP kinase signaling, suppressing c-Myc expression, or inhibiting telomerase activity, caused telomere dysfunction and proliferative defects in cells that had escaped senescence, whereas ectopic expression of hTERT facilitated OIS escape. In human early neoplastic skin and breast tissue, hTERT expression was detected in cells that displayed features of senescence, suggesting that reactivation of telomerase expression in senescent cells is an early event during cancer progression in humans. Together, our data demonstrate that cells arrested in OIS retain the potential to escape senescence by mechanisms that involve derepression of *hTERT* expression.

oncogene-induced senescence | telomerase | telomere | senescence escape | TERT

Many cancers develop by an evolutionary process as genetic and epigenetic changes accumulate in somatic cells, allowing these cells to escape the restraints imposed by tumor suppressive pathways. In recent years, it has become evident that one critical barrier to cancer progression is a proliferative arrest termed cellular senescence. We and others have demonstrated that the reasons for the inactive nature of certain human cancer precursor lesions is because cells within these lesions had undergone cellular senescence (1, 2). However, given that these early and inactive neoplasms occasionally progress to more advanced cancer stages, it is possible that cells can escape senescence after a prolonged period in a seemingly stable arrested state.

Cellular senescence is generally thought to be an irreversible proliferative arrest, activated in response to numerous cell intrinsic and extrinsic signals and stresses (3). In mammals, a primary function of cellular senescence is to suppress cancer development; however, other roles for this stress response have also emerged in recent years (4). Oncogene-induced senescence (OIS) is a response of cells encountering strong oncogenic signals, such as those initiated by mutant and constitutively active H-Ras^{G12V} (5) or the downstream effector kinase B-Raf^{V600E} (6). These oncogenes constitutively activate a mitogen-activated protein (MAP) kinase signaling pathway, which leads to an unregulated transcriptional activation and stabilization of growth promoting genes including *c-Myc* (7). Because of resulting hyperproliferative signals, cells encounter a high degree of DNA replication stress and, as a result, develop numerous double-stranded DNA breaks (DSBs) that occur primarily at fragile sites. The ensuing DNA damage response (DDR) triggers OIS, thereby arresting cells within a few cell-division cycles after oncogene expression (8, 9). Although most DSBs in arrested cells are eventually resolved by cellular DSB repair processes, some persist and consequently convert the otherwise transient DDR into a more permanent growth arrest. We and others have demonstrated that the persistent DDR is primarily telomeric, triggered by irreparable telomeric DSBs (1, 10, 11).

Expressing oncogenes in normal human cells results in large-scale chromatin rearrangements, culminating in the formation of senescence-associated heterochromatin foci (SAHFs). Initially identified by DAPI staining, SAHFs are highly condensed regions of individual chromosomes that are enriched in heterochromatin proteins (12, 13). Although previously thought to be structures exclusive to senescent cells, more recent studies have demonstrated that SAHFs are features of cells expressing oncogenes, regardless of whether they are proliferating or senescent (14). In senescent cells, however, E2F target genes appear to reside within SAHFs, whereas sites of active RNA transcription are excluded from these structures. These observations suggest that one function of SAHF formation is to repress expression of growth-promoting genes during cellular senescence (12, 13, 15).

Previously, we demonstrated that dysfunctional telomeres stabilize OIS (1). Telomeres are long and repetitive DNA sequences that, together with components of the telomeric protein complex shelterin, suppress DNA repair activities at the ends of linear chromosomes. Telomere length, however, is not static. With every cell-division cycle, telomeres progressively erode, primarily because of the inability of cellular DNA polymerases to efficiently replicate repetitive chromosome ends. Once they are critically short, telomeres become dysfunctional and consequently activate a persistent

Significance

Normal cells respond to oncogenic signals by activating cellular senescence, a state of irreversible/permanent growth arrest that prevents cells from undergoing further cell divisions. Although this oncogene-induced senescence (OIS) is considered a critical tumor-suppressive mechanism, the irreversible nature of OIS remains controversial. In this study, we demonstrate that OIS is not always stable. After a prolonged period in senescence, cells can re-enter the cell-division cycle with epigenetic changes that facilitate cell transformation. Escape from OIS was promoted by derepression of *hTERT* gene expression, an enzyme that provides cellular immortality and is activated in >90% of human cancers.

Author contributions: U.H. designed research; P.L.P. performed research; A.S., N.M., and O.B. contributed new reagents/analytic tools; P.L.P. analyzed data; and P.L.P. and U.H. wrote the paper.

The authors declare no conflict of interest.

This article is a PNAS Direct Submission.

Freely available online through the PNAS open access option.

[1]To whom correspondence should be addressed. Email: herbigut@njms.rutgers.edu.

This article contains supporting information online at www.pnas.org/lookup/suppl/doi:10.1073/pnas.1602379113/-/DCSupplemental.

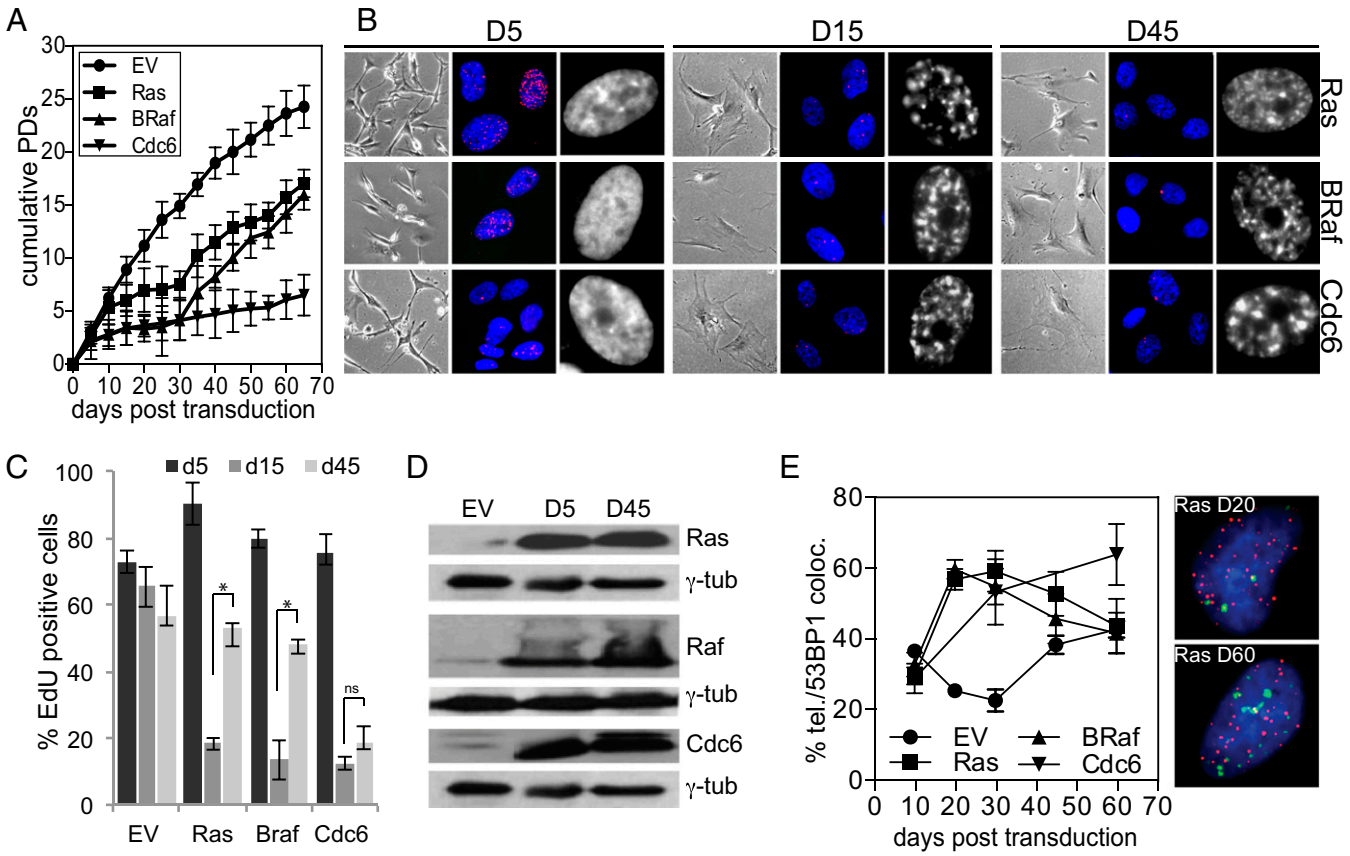

Fig. 1. Human cells can escape OIS after an extended period in a growth-arrested state. (*A*) Proliferation curve of BJ cells transduced with H-Ras^{G12V} (Ras), B-Raf^{V600E} (BRaf), Cdc6, and empty vector control (EV). Values are expressed as mean ± SD. Cumulative population doublings (PDs) were calculated at each passage ($n = 3$). (*B*) Representative images of cells displaying changes in morphology (left column), 53BP1 foci (red, center column), and SAHF (single nucleus shown; right column) at indicated days (D) after oncogene transduction. (*C*) Percentage of EdU-positive cells (±SD) at indicated days after oncogene transduction ($n = 3$). EdU was added for 48 h before analysis. *$P < 0.05$ by unpaired *t* test. (*D*) Immunoblot showing expression of Ras, B-Raf, and Cdc6 in BJ cells at indicated days after transductions. γ-tubulin served as a loading control. (*E*) Percentage of 53BP1 foci colocalizing with telomeric DNA at indicated days after oncogene transduction, as measured by telomere immunoFISH. A minimum of 50 DDR-positive cells were analyzed for each group and each time point. Representative images of Ras-expressing cells stained 53BP1/telomere colocalizations at indicated days are shown: 53BP1 (green), telomere (red), and nuclear DNA (blue).

DDR, which ultimately leads to telomere dysfunction-induced cellular senescence (TDIS) (16, 17). Dysfunctional telomeres are also generated in the absence of significant telomere shortening. For example, genotoxic stresses that cause breaks in double-stranded DNA, such as DNA replication stress, also generate dysfunctional telomeres and trigger TDIS if such breaks occur in telomeric repeats (10, 11). In fact, telomeres are particularly prone to DNA breakage because they resemble fragile sites (18, 19). Because oncogenes such as H-Ras^{G12V} and B-Raf^{V600E} cause DNA replication stress, they also generate dysfunctional telomeres in somatic human cells. Importantly, the generation of such dysfunctional telomeres is critical to stabilize an otherwise transient proliferative arrest in H-Ras^{G12V}– and B-Raf^{V600E}–expressing human somatic cells (1, 20).

To counteract progressive telomere erosion and replication stress-induced telomeric DSBs, stem and progenitor cells, as well as a great majority of cancer cells, express telomerase. Consisting of two core components, a catalytic subunit hTERT and a template RNA component hTR, telomerase counteracts telomere shortening by adding de novo telomeric repeats to chromosomal ends (21). In somatic human cells, however, transcription of telomerase is suppressed because of a repressive chromatin state at the *hTERT* promoter (22, 23). In contrast, cancer cells display a pattern of active chromatin marks surrounding the *hTERT* promoter, thereby allowing transcription factors such as c-Myc to promote expression of the *hTERT* gene (24). Recently discovered *hTERT* promoter mutations in human cancer cells have been demonstrated to alter the local epigenetic landscape from a repressive state to open and transcriptionally active chromatin, providing a mechanism that may act as an epigenetic switch at the *hTERT* promoter (25). However, because most cancers reactivate *hTERT* gene expression independent of promoter mutations (26), other and currently unknown mechanisms must exist that promote epigenetic changes and create an active chromatin state at the *hTERT* promoter during cancer development in humans.

Although OIS is a critical tumor-suppressing mechanism in mammals, whether it truly presents a stable and irreversible barrier to cancer progression is unclear. In this study we have characterized the long-term stability of a proliferative arrest induced by overexpression of the oncogenes H-Ras^{G12V}, B-Raf^{V600E}, and Cdc6 and reveal that, depending on the signaling pathways activated, cells can escape OIS after a prolonged period of inactivity. Escape from OIS was due to a combination of events, including a MAP kinase-mediated stabilization of c-Myc expression, derepression of the *hTERT* promoter, and an ensuing reactivation of telomerase. Importantly, senescent cells of human melanocytic skin and breast lesions showed enhanced hTERT expression at early stages during cancer development, suggesting that escape from senescence, facilitated by telomerase reactivation, contributes to cancer progression in humans.

Results

Cells Can Escape OIS After a Prolonged Period in Senescence. We previously demonstrated that OIS, induced by constitutively active

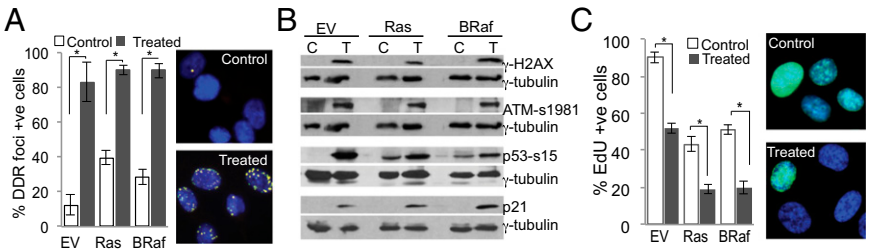

Fig. 2. The DDR is intact in cells that had escaped OIS. BJ cells expressing H-Ras^{G12V} and B-Raf^{V600E} were treated with 6 μg/mL Zeocin for 4 h. (*A*) Quantitation of DDR-positive cells (±SD), defined as a cell nucleus with at least three colocalizations between γH2AX (green) and 53-BP1 (red). Nuclei were counterstained by using DAPI (blue). At least 150 cells were quantified for each group. *$P < 0.05$; by paired *t* test ($n = 3$). Micrographs show representative images of cells treated with Zeocin (*A*, *Right Lower*) or control treated cells (*A*, *Right Upper*) and immunostained using anti-53BP1 (red) and γH2AX (green) antibodies. (*B*) Immunoblots showing levels of indicated DDR factors in control (C) and Zeocin (T)-treated cultures. γ-tubulin served as a loading control. BRaf, cells that had escaped B-Raf^{V600E}–induced senescence; EV, presenescent cells expressing EV; Ras, cells that had escaped H-Ras^{G12V}–induced senescence. (*C*) Percentage of EdU-positive cells (±SD) after control and Zeocin treatment for 2 h. EdU was incorporated for 48 h. *$P < 0.05$ by paired *t* test ($n = 3$). Micrographs show representative images of EdU (green)-positive cells. Nuclei were counterstained by using DAPI (blue).

H-Ras^{G12V} and B-Raf^{V600E}, is triggered as a consequence of DNA replication stress-induced DSBs and stabilized because of the persistence of telomeric DSBs (1). To test the long-term stability of OIS, we retrovirally transduced three oncogenes, H-Ras^{G12V}, B-Raf^{V600E}, and Cdc6, into somatic human cells and monitored proliferation rates over a period of 2 mo. Consistent with previous data, oncogene-expressing cells ceased proliferation 5–10 d after retroviral transduction, as demonstrated by proliferation curves and 5-ethynyl-2′-deoxyuridine (EdU) incorporation assays. Arrested cells displayed an enlarged and flattened morphology and numerous DDR foci, as well as SAHF, demonstrating that cells had undergone OIS (Fig. 1 *A*–*C*).

As we continued to maintain these essentially senescent cells with regular medium changes in culture, we observed at various frequencies that H-Ras^{G12V}– and B-Raf^{V600E}–expressing cells eventually continued to proliferate, despite retaining high oncogene expression levels, SAHF, and a senescence-like morphology suggesting that they had escaped OIS (Fig. 1 *A*–*D*). Analysis at the single-cell level revealed that actively proliferating cells, those that incorporated EdU, retained H-Ras and B-Raf expression, often at levels higher compared with nonproliferating cells in the same culture (Fig. S1*A*). Overall, 17 of 33 (52%) H-Ras^{G12V} transductions and 6 of 17 (35%) B-Raf^{V600E} transductions displayed this pattern of senescence induction and escape. Continued proliferation of the cultures was not due to clonal expansion of one or a few cells that had inactivated the senescence program; rather, it was a consequence of a larger fraction of cells (>10%) that consistently started to proliferate throughout the entire senescent culture at approximately day 28 after oncogene transduction, as demonstrated by EdU incorporation assays (Fig. S1*B*). Similar kinetics of OIS escape were also observed in primary human fibroblast GM21, but not in HSF43, suggesting that not all cell strains are susceptible to OIS escape (Fig. S1*C*). In contrast to H-Ras^{G12V}– and B-Raf^{V600E}–expressing cells, all six transductions conducted by using Cdc6-expressing retrovirus (100%) resulted in senescent cultures in which all cells remained stably arrested for at least 2 mo, in all three cell strains tested (Fig. 1 *A* and Fig. S1*C*). Our data therefore demonstrate that OIS is not always stable and that cells displaying all of the characteristics of senescence retain the potential to re-engage proliferation after a prolonged period in a senescence-arrested state.

To characterize the causes for senescence escape in H-Ras^{G12V}– and B-Raf^{V600E} expressing cells, we measured telomere dysfunction as cells entered, remained, and escaped OIS by telomere-immunoFISH (Fig. 1*E* and Fig. S1*D*). Seven days after transducing oncogenes into somatic human cells, just as cells entered OIS, most DDR foci did not colocalize with telomeric repeats, which was consistent with our previous data (1). As cells remained growth-arrested, between days 10 and 30 after transduction, nontelomeric DDR foci were progressively resolved, whereas telomeric DDR foci persisted. This repair of nontelomeric DDR foci resulted in an overall increase in the percentage of 53BP1–telomere colocalizations, also termed telomere dysfunction-induced DNA damage foci (TIF), in the senescent cell population (Fig. 1*E*). However, as H-Ras^{G12V}– and B-Raf^{V600E}–expressing cells escaped OIS, at 30 d after transduction of the oncogenes, telomeric DDR foci also progressively declined in abundance. In contrast, Cdc6-overexpressing cells that were stably arrested continued to resolve primarily nontelomeric DDR foci, which resulted in a further increase in 53BP1–telomere colocalizations during the time period analyzed (Fig. 1*E* and Fig. S1*D*).

Cells That Escaped OIS Retain Functional DDRs. A progressive reduction of telomeric DDR foci during the period of senescence escape could also suggest that H-Ras^{G12V}– and B-Raf^{V600E}–expressing cells acquired changes that inactivate the DDR, thereby suppressing DNA damage checkpoints and DNA repair activities. Indeed, OIS can be bypassed by inactivating a number of DDR and repair factors (8, 9). To test the possibility that cells continued to proliferate because of DDR inactivation, we treated cells that had escaped OIS with Zeocin, a potent inducer of DSBs. Activation of the DNA damage checkpoint was monitored by immunofluorescence analysis of DDR foci formation, immunoblotting against DDR factors, and EdU incorporation assays. Four hours after Zeocin treatment, >80% of H-Ras^{G12V}– and B-Raf^{V600E}–overexpressing cells displayed a minimum of three DDR foci per cell nucleus, similar to control cells transduced with empty vector (EV) (Fig. 2*A*). This increase in DDR foci was in contrast to untreated cells that infrequently displayed DDR foci. Similarly, activation of the DDR was equally efficient in Zeocin-treated EV, H-Ras^{G12V}–, and B-Raf^{V600E}–overexpressing cells, as demonstrated by immunoblotting against γ-H2AX, ATM-S1981, phosphor-p53-S15, and p21 (Fig. 2*B*). Finally, incorporation of EdU into nuclear DNA was significantly decreased in both control and oncogene-expressing cells upon drug treatment, overall demonstrating that cells that had escaped OIS retained the ability to undergo a DNA damage checkpoint arrest, similar to normal somatic human cells (Fig. 2*C*).

Escape from OIS Is a Consequence of Telomerase Reactivation. We previously demonstrated that H-Ras^{G12V}– and B-Raf^{V600E}–induced senescence can be destabilized by ectopic expression of the catalytic subunit of telomerase hTERT before senescence induction (1). By suppressing DNA replication stress-induced DSB formation in telomeric repeats, hTERT-expressing cells did not acquire persistent telomeric DDR foci and thus continued to proliferate after a transient arrest that lasted for ∼1 wk. Because hTERT overexpression

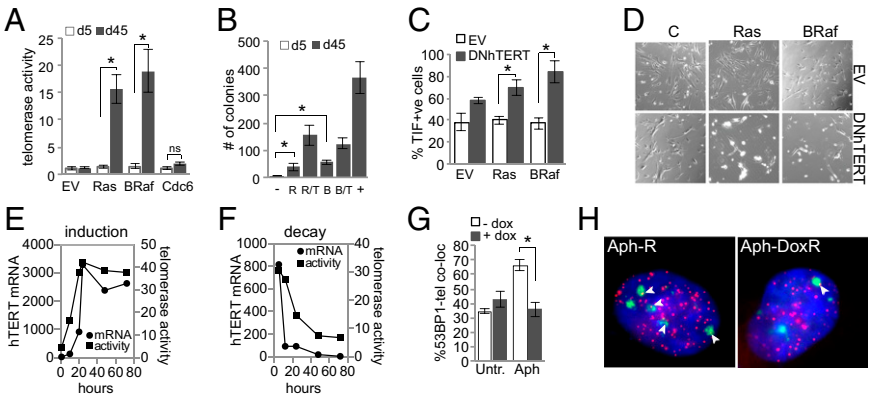

Fig. 3. Spontaneous reactivation of telomerase activity is necessary and sufficient to promote cell proliferation in cells that had escaped OIS because of its ability to resolve telomeric DDR foci. (*A*) Relative telomerase activity (±SD) in BJ cells expressing H-Ras^{G12V} and B-Raf^{V600E} at indicated days (d) after transduction, as measured by TRAPeze assay. *$P < 0.05$ by unpaired *t* test; ns, not significant ($n = 3$). (*B*) Induction of anchorage-independent growth in BJ cells that escaped H-Ras^{G12V}–induced (R) and B-Raf^{V600E}–induced (B) senescence (d45) in the absence and presence of SV40 large T-antigen (T), as measured by using soft agar colony-forming assay. (+) positive control, BJ cells expressing H-Ras^{G12V}, hTERT from a retroviral promoter, and SV40 large T antigen. *$P < 0.05$ by ANOVA ($n = 3$). (*C*) Percentage of telomere dysfunction induced foci (TIF)-positive cells (±SD) in cells that escaped H-Ras^{G12V}– and B-Raf^{V600E}–induced senescence 5 d after transduction of a dominant defective version of hTERT (DNhTERT) or an EV control. A cell was considered TIF-positive when, in a given cell nucleus, ≥50% of 53BP1 foci colocalized with telomeric repeats. A minimum of 50 cells were analyzed for each group. *$P < 0.05$ by unpaired *t* test ($n = 3$). (*D*) Phase contrast images illustrating morphological changes in cells that had escaped H-Ras^{G12V}– and B-Raf^{V600E}–induced senescence 10 d after transduction with DNhTERT. (*E*) Time-dependent response curve of hTERT mRNA expression levels and activity in cells expressing hTERT from a dox-responsive promoter after treatment with 100 ng/mL dox, as measured by RT-qPCR and TRAPeze, respectively. (*F*) Time-dependent recovery curve of telomerase activity after removal of dox. (*G*) Percentage of TIF-positive cells expressing dox-responsive hTERT (±SD). Aph, cells treated with 0.5 μM aphidicolin for 48 h; +dox, after the 48-h treatment with aphidicolin, dox was added for an additional 48 h; Untr, untreated cells. A minimum of 50 cells were analyzed for TIF and for each treatment. *$P < 0.05$ by unpaired *t* test ($n = 3$). (*H*) Micrographs show representative images of cells displaying TIF at time of analysis: γH2AX (green), telomere (red), and nuclear DNA (blue). Arrows indicate colocalizations of γH2AX with telomeres.

destabilizes OIS, we tested the possibility that senescence escape in H-Ras^{G12V}– and B-Raf^{V600E}–expressing cells was due to activation of endogenous telomerase activity. Telomerase activity was measured by TRAPeze assay before cells entered OIS (day 5 after transduction) and after cells escaped OIS (day 45 after transduction). A dramatic and significant increase in telomerase activity was indeed detected in H-Ras^{G12V}– and B-Raf^{V600E}–expressing cells that had escaped OIS, but not in control and Cdc6-expressing cells at any time point tested (Fig. 3*A* and Fig. S2 *A* and *B*). Endogenous telomerase activity was sufficient to allow continuous proliferation of H-Ras^{G12V}– and B-Raf^{V600E}–expressing cells beyond day 200 after transduction and promoted robust colony formation in soft agar colony formation assays (Fig. 3*B* and Fig. S2*C*). Our data therefore suggest that escape from OIS was a consequence of spontaneous activation of endogenous telomerase activity.

A primary function of hTERT is to add de novo telomeric repeats to short telomeres by using its reverse transcriptase activity and thereby prevent critical telomere erosion, telomere dysfunction, and consequently, TDIS. Telomerase, however, also possesses noncanonical functions that promote cell proliferation and that are independent of its telomeric role. To discern which of these functions is promoting OIS escape, we overexpressed a dominant defective mutant of hTERT (DN-hTERT) in cells that had escaped senescence, to specifically inhibit telomerase reverse-transcriptase activity, while leaving the noncanonical functions of hTERT intact (Fig. S2*D*) (27). In line with previous observations, expression of DN-hTERT in normal somatic human cells did not cause immediate proliferative defects, although a modest increase in cells displaying dysfunctional telomeres was detected (Fig. 3*C*). An increase in dysfunctional telomeres following inhibition of hTERT is consistent with a proposed role of hTERT in facilitating telomere replication during the S-phase of the cell cycle in normal human somatic cells (28). Expression of DN-hTERT in cells that had escaped OIS, however, triggered a significantly more robust telomeric DDR, and cells lost viability just 10 d after transduction of the mutant (Fig. 3 *C* and *D*). Consistent with our published data demonstrating that oncogenes cause telomeric replication defects and telomere dysfunction in normal somatic human cells (1), inhibition of telomerase activity in cells that had escaped H-Ras^{G12V}– and B-Raf^{V600E}–induced senescence caused rapid and stochastic telomere attrition that was even more severe compared with presenescent cells expressing these oncogenes (Fig. S2*E*). The primary function of telomerase in cells that had escaped H-Ras^{G12V}– and B-Raf^{V600E}–induced senescence therefore is to prevent stochastic telomere loss and to suppress a telomeric DDR that would otherwise be generated as a result of oncogene-induced DNA replication stress.

The reduction of TIF in cells that had reactivated telomerase activity suggests that telomerase can repair dysfunctional telomeres, thereby destabilizing OIS. To determine whether hTERT has the ability to resolve TIF after they had been generated, we developed an inducible hTERT (iTERT) expression system in human somatic fibroblasts GM21 in which telomerase expression and activity can be switched on and off by the addition and removal of doxycycline (dox), respectively (Fig. S3*A*). Analysis of the kinetics of induction revealed that iTERT mRNA and telomerase activity reach maximum levels 24 h after dox addition, whereas removal of the drug resulted in a progressive decline of iTERT mRNA and telomerase activity, returning to background levels after just 36 h in dox-free medium (Fig. 3 *E* and *F*). To cause replication stress-induced telomere dysfunction, we treated cells with low levels of aphidicolin for 48 h, which generated both nontelomeric and telomeric DDR foci (Fig. S3 *B* and *C*), followed by a recovery period in aphidicolin-free medium for an additional 48 h. During the recovery period, cells resolved primarily nontelomeric DDR foci, thereby enriching them for persistent telomeric ones, or TIF. In the absence of iTERT induction, this procedure resulted in a greater than twofold increase in telomeric DDR foci (Fig. 3*G*). Significantly, inducing iTERT expression during the recovery period, after TIF had been generated, reduced the percentages of telomeric DDR foci in the cell population by 45% (Fig. 3 *G* and *H*). Our data therefore demonstrate that telomerase can resolve telomeric DDR foci that are generated as a consequence of DNA replication stress.

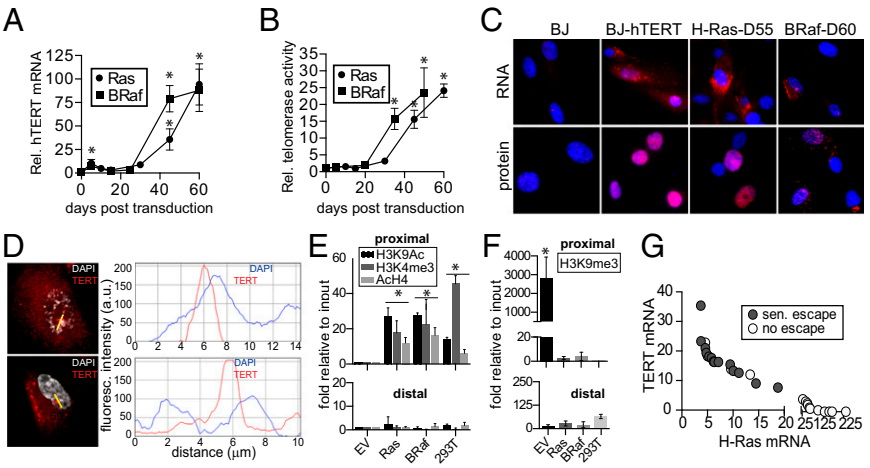

Fig. 4. High telomerase activity in cells that had escaped OIS is due to transcriptional activation of hTERT mRNA expression in chromatin regions that are excluded from SAHF and enriched with active chromatin marks. (*A*) Time course analysis of hTERT mRNA expression in BJ cells retrovirally transduced with H-Ras^{G12V} (Ras) and B-Raf^{V600E} (BRaf) as measured by RT-qPCR. Data were normalized to GAPDH levels, and fold expression was compared with BJ-EV. *$P < 0.05$ by unpaired *t* test ($n = 3$). (*B*) Time course analysis of telomerase activity in BJ cells transduced with H-Ras^{G12V} (Ras) and B-Raf^{V600E} (BRaf) as measured by TRAPeze. *$P < 0.05$ by unpaired *t* test ($n = 3$). (*C*) RNA-FISH analysis of hTERT mRNA levels (*Upper*) and protein levels detected by immunostaining (*Lower*) in normal fibroblasts (BJ), cells overexpressing hTERT from a transgene (BJ-hTERT), an cells that has escaped H-Ras^{G12V}–induced (H-Ras-D55) and B-Raf^{V600E}–induced (BRaf-D60) senescence. Note that imaging exposure times for hTERT-transduced cells (BJ-hTERT) were significantly shorter compared with the other cells shown. (*D*, *Left*) hTERT RNA-FISH (red) in cells that had escaped H-Ras^{G12V}–induced (*Upper*) and B-Raf^{V600E}–induced (*Lower*) senescence. SAHF were visualized by using DAPI staining (white). (*D*, *Right*) Quantification of DAPI (blue) and hTERT mRNA (red) signal intensities across the indicated line in images in *D*, *Left*. (*E*) Relative enrichment levels of euchromatin markers H3K4Me3, H3K9Ac, and AcH4 at the hTERT proximal (*Upper*) promoter and distal (*Lower*) promoter as analyzed by using ChIP-qPCR. *$P < 0.05$ by unpaired *t* test ($n = 3$). (*F*) CHIP-qPCR analysis of trimethylated H3K9 at the hTERT proximal (*Upper*) promoter and distal (*Lower*) promoter. *$P < 0.05$ by unpaired *t* test ($n = 3$). (*G*) Scatter plot of hTERT mRNA levels compared with H-Ras^{G12V} mRNA levels for a total of 30 individual experiments. ●, cultures that had escaped H-Ras^{G12V}–induced senescence; ○, cultures that remained senescent beyond 30 d after entry into OIS.

High Telomerase Activity in Cells That Had Escaped OIS Is Due to Derepression of *hTERT* mRNA Expression. An increase in telomerase activity at the time of OIS escape could be due to a number of reasons. For example, although *hTERT* is regulated primarily at the transcriptional level, its enzymatic activity can also be modulated by posttranslational modifications or holoenzyme assembly, among other mechanisms (29). To test whether increased telomerase activity in cells that had escaped OIS was a result of increased *hTERT* expression, we measured mRNA levels in H-Ras^{G12V}– and B-Raf^{V600E}–expressing cells by quantitative RT-PCR (RT-qPCR) at regular intervals after oncogene transduction. Although hTERT mRNA levels could not be detected in control EV expressing somatic human cells, a modest, yet statistically significant, increase in hTERT mRNA was detected in H-Ras^{G12V}–expressing cells 1 and 5 d after transduction, the period before undergoing OIS (Fig. 4*A*). Similar results were obtained in B-Raf^{V600E}–expressing cells. This modest increase in hTERT mRNA levels, however, was not associated with an increase in telomerase activity (Fig. 4*B*). Between days 10 and 30, as cells remained in a senescent state, no significant increase in hTERT mRNA levels or telomerase activity could be detected. In contrast, at the time when H-Ras^{G12V}– and B-Raf^{V600E}–expressing cells escaped OIS, hTERT mRNA levels and telomerase activity increased progressively and dramatically and reached levels of 95- and 25-fold above controls, respectively, at day 60 after transduction of the oncogenes (Fig. 4 *A* and *B*). In cells that had escaped OIS, hTERT mRNA levels and telomerase activity were well within the range of five commonly studied cancer cell lines (Fig. S4 *A* and *B*). Furthermore, lentivirus-mediated overexpression of hTERT in fully senescent H-Ras^{G12V}–expressing cells potentiated escape from OIS, demonstrating that hTERT expression and increased telomerase activity in senescent cells are a driver, and not a consequence, of senescence escape (Fig. S4*C*).

Analysis of mRNA expression levels on the single cell level using RNA-FISH revealed a heterogeneous and mosaic *hTERT* gene expression pattern. Although some cells expressed very low amounts of hTERT mRNA, others, including those with large cell nuclei as well as prominent and discrete SAHF, displayed high levels of hTERT mRNA (Fig. 4*C*). A similar staining pattern was observed by using an antibody specific to hTERT protein (Fig. 4*C*). This heterogeneity in hTERT expression levels was in contrast to cultures that expressed *hTERT* from a transgene, in which all cells expressed similar levels of hTERT, based on the staining intensity of the RNA-FISH probe and anti-hTERT antibodies (Fig. 4*C* and Fig. S4*D*). Transcriptionally active alleles of *hTERT*, characterized by a discrete and prominent focus within the cell nucleus, did not overlap with SAHF, but, rather, localized to their periphery, suggesting that the *hTERT* promoter resides outside of senescence-associated heterochromatic regions in cells that had escaped OIS (Fig. 4*D*). Indeed, although the *hTERT* promoter in somatic cells is in a repressive chromatin state (23), cells that had escaped OIS displayed an active chromatin state characterized by the presence of H3K9Ac, H3K4me3, and AcH4, but absence of the repressive mark H3K9me3, as demonstrated by quantitative ChIP (qChIP) (Fig. 4 *E* and *F*). Thus, our data not only demonstrate that the increase in hTERT mRNA levels, protein levels, and telomerase activity coincides precisely with the time of OIS escape, but they also suggest that H-Ras^{G12V}– and B-Raf^{V600E}–expressing cells can escape OIS as a result of chromatin changes that permit transcriptional activation of the *hTERT* gene.

Because not all oncogene transductions resulted in senescent cultures that eventually escaped OIS, we tested whether the long-term stability of OIS was dependent on expression levels of hTERT. As demonstrated in Fig. 4*G*, none of the transduced cell cultures in which hTERT mRNA levels were less than eightfold above normal levels were able to escape OIS. In addition, none of the senescent cell cultures that displayed H-Ras levels >20-fold above those of endogenous H-Ras escaped OIS. Our data therefore suggest that OIS becomes unstable only when telomerase expression reaches levels that are high enough to repair

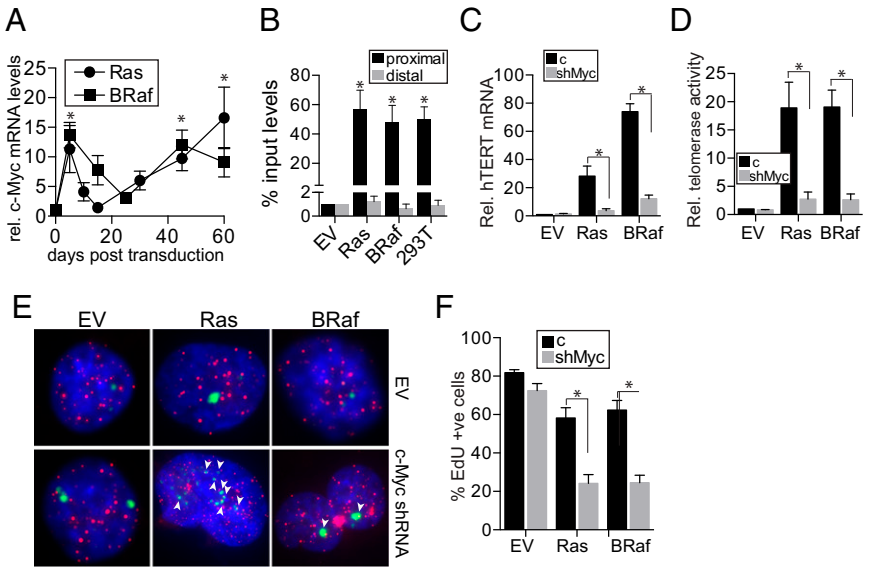

Fig. 5. Increased hTERT expression and telomerase activity in cells that had escaped OIS is a direct consequence of high c-Myc levels. (*A*) Time course analyses of c-Myc mRNA levels (±SD) in cells that were retrovirally transduced with H-Ras^{G12V} (Ras; $n = 4$) and B-Raf^{V600E} (BRaf; $n = 3$) as measured by RT-qPCR. Data were normalized to GAPDH levels, and fold expression was compared with cells expressing EV controls. *$P < 0.05$ by unpaired *t* test ($n = 3$). (*B*) ChIP analysis of c-Myc binding to hTERT proximal promoter and distal promoter regions. Error bars represent mean ± SD. *$P < 0.05$ by unpaired *t* test ($n = 3$). (*C* and *D*) Relative hTERT mRNA levels as measured by RT-qPCR (*C*) and telomerase activity as measured by TRAPeze (*D*) in cells that had escaped H-Ras^{G12V}–induced (Ras) and B-Raf^{V600E}–induced (BRaf) senescence and that were subsequently transduced with c-Myc shRNA (shMyc) or control shRNA for 5 d. Error bars represent ± SD. *$P < 0.005$ by unpaired *t* test ($n = 3$). (*E*) Representative images showing dysfunctional telomeres, indicated by arrows, in cultures that had escaped OIS and that were subsequently transduced with c-Myc shRNA for 10 d: γH2AX (green), telomere (red), and nuclear DNA (blue) counterstained with DAPI. (*F*) Percentage of EdU-positive cells (±SD) in cultures that had escaped OIS and that were subsequently transduced with c-Myc shRNA for 10 d. EdU was incorporated at least for 48 h, and a minimum of 150 cells were quantified per group. *$P < 0.05$ by unpaired *t* test ($n = 3$).

existing TIF and suppress formation of new dysfunctional telomeres generated as a result of oncogene-induced DNA replication stress.

Transcriptional Activation of *hTERT* Expression in Cells That Had Escaped OIS Is a Consequence of MAP Kinase-Dependent Regulation of c-Myc Levels. A number of transcription factors have been demonstrated to activate expression of hTERT mRNA in mammalian cells (30). One transcription factor that not only regulates hTERT expression, but also is frequently amplified in human cancer, is c-Myc (23). Analysis of c-Myc mRNA levels by RT-qPCR revealed a spike of expression that was significantly higher compared with proliferating control cells soon after transducing the oncogenes H-Ras^{G12V} and B-Raf^{V600E} and as these cells were in a hyperproliferative state (Fig. 5*A*). As cells entered and remained in senescence, 10–25 d after transduction, c-Myc mRNA levels declined, yet they remained higher compared with proliferating control cells at all times analyzed. At the time of senescence escape, and coinciding precisely with hTERT mRNA expression (Fig. 4*A*), c-Myc mRNA expression further increased, reaching levels that were 10- to 15-fold greater compared with controls. Lentiviral transduction of shRNA targeting *c-Myc* at day 18 after H-Ras^{G12V} transduction stabilized OIS, demonstrating a direct involvement of c-Myc in escape from OIS (Fig. S5 *A* and *B*). Furthermore, given the synchronous timing of progressively increasing c-Myc and hTERT expression levels as cells escaped OIS, our data suggest that c-Myc may be directly involved in transcriptional activation of the endogenous *hTERT* promoter in cells that had escaped OIS. Indeed, we demonstrate that c-Myc directly and specifically associates with the *hTERT* promoter in cells that had escaped OIS, but not in controls, as demonstrated by qChIP analysis (Fig. 5*B*).

To directly test whether c-Myc transactivates *hTERT* expression, we suppressed its levels in cells that had escaped OIS by using shRNA (Fig. S5*A*). Significantly, stable knockdown of c-Myc dramatically reduced hTERT mRNA expression levels (Fig. 5*C*), reduced telomerase activity to background levels (Fig. 5*D*), and rapidly triggered TDIS in cells that had escaped OIS, but not in controls (Fig. 5 *E* and *F*). Our data therefore demonstrate that spontaneous activation of *hTERT* expression as well as activity is a

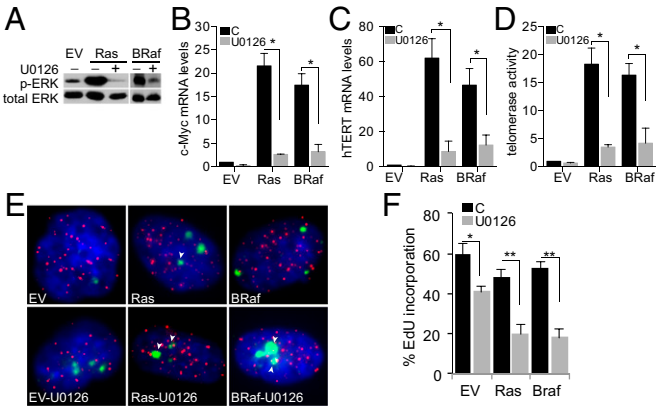

Fig. 6. The MAP kinase inhibitor U0126 reduces c-Myc expression levels resulting in low telomerase activity, telomere dysfunction, and cellular senescence in cells that had escaped OIS. (*A*) Immunoblots showing reduction of phospho-ERK in indicated cultures that were treated with 10 μM U0126 (+) or vehicle control (–) for 16 h. (*B* and *C*) Relative c-Myc (*B*) and hTERT (*C*) mRNA levels (±SD) in indicated cultures after U0126 treatment, as measured by RT-qPCR. *$P < 0.05$ by paired *t* test ($n = 3$). (*D*) Relative telomerase activity (±SD) in indicated cultures after U0126 treatment. *$P < 0.05$ by paired *t* test ($n = 3$). (*E*) Representative images showing dysfunctional telomeres, indicated by arrows, in cells treated with 10 μM U0126: γH2AX (green), telomere (red), and nuclear DNA (blue). (*F*) Percentage of EdU-positive cells (±SD) treated with 10 μM U0126. EdU was added at least for 48 h, and a minimum of 150 cells were quantified. *$P = 0.02$; **$P < 0.007$ by paired *t* test ($n = 3$). Braf, cells that had escaped B-Raf^{V600E}–induced senescence; Ras, cells that had escaped H-Ras^{G12V}–induced senescence.

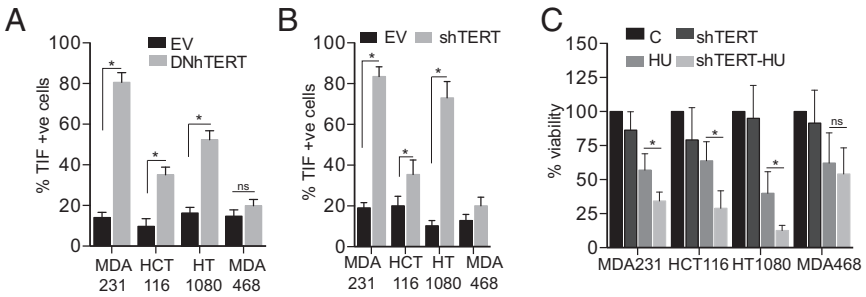

Fig. 7. Inhibition of telomerase in cancer cell lines harboring Ras/B-Raf mutations causes telomere dysfunction and increases their sensitivity to the cytotoxic drug hydroxyurea (HU). (*A* and *B*) Indicated cancer cell lines were transduced with a dominant-negative form of hTERT, DNhTERT (*A*), or an shRNA-targeting hTERT (*B*), and the percentage of TIF-positive cells (±SD) was quantitated by analyzing telomere–γH2AX colocalizations 3 wk after transduction. **P* < 0.05 by unpaired *t* test (*n* = 3). (*C*) Percent viability (±SD) of indicated cancer cell lines transduced with a control shRNA (c), shRNA-targeting hTERT (shTERT), treated with 150 μM hydroxyurea for 4 d, or a combination of shTERT and HU. ns, not significant. **P* < 0.05 by paired *t* test (*n* = 3).

direct consequence of high c-Myc expression levels in cells that had escaped H-Ras^{G12V}– and B-Raf^{V600E}–induced senescence.

Signaling through the H-Ras and B-Raf MAP kinase pathway can regulate *c-Myc* expression and protein stability, thereby promoting transactivation of a number of c-Myc–regulated genes (7). Not surprisingly, cells that had escaped H-Ras^{G12V}– and B-Raf^{V600E}–induced senescence and continued proliferating with high oncogene levels also displayed hyperphosphorylated MAP kinase ERK, in addition to high c-Myc and hTERT levels, demonstrating a constitutively active MAP kinase signaling pathway in these cells (Fig. 6*A*). Pharmacological inhibition of this pathway by using U0126, a specific inhibitor of the upstream MAP kinase MEK1/MEK2 that did not affect expression of H-Ras and B-Raf (Fig. S6*A*), not only stabilized OIS when added to senescent cell cultures before escape (Fig. S6*B*), but it also diminished phosphorylation of ERK and reduced c-Myc and hTERT mRNA expression to almost background levels in cells that had escaped OIS (Fig. 6 *B* and *C*). In these cells, treatment with U0126 resulted in low telomerase activity (Fig. 6*D*), promoted rapid telomere dysfunction (Fig. 6*E*), and caused cells to re-enter cellular senescence as demonstrated by EdU incorporation assays (Fig. 6*F*). Our data therefore demonstrate that constitutive MEK/ERK MAP kinase signaling promotes escape from OIS and that expression and activity of hTERT is dependent on an active Ras/B-Raf MAP-kinase signaling pathway in cells that had escaped OIS.

Cancer Cells with Deregulated ERK/MAP Signaling Pathway Are Sensitive to Telomerase Inhibition. The observations that H-Ras^{G12V}– and B-Raf^{V600E}–expressing cells depend on high telomerase activity to suppress rapid TIF formation and promote cell survival (Fig. 3) raises the possibility that cancer cells with deregulated MAP kinase signaling pathways are sensitive to telomerase inhibition. Indeed, the colon cancer cell lines HCT116 and the fibrosarcoma cell line HT1080, as well as the breast cancer cell line MDA-231, all harboring Ras/B-Raf mutations (Fig. S7*A*), were sensitive to hTERT inhibition using either DN-hTERT or shRNA targeting hTERT and developed dysfunctional telomeres 3 wk after treatment (Fig. 7 *A* and *B*, and Fig. S7 *B*–*D*). In contrast, the cancer cell line MDA468 with characterized mutation in the PTEN signaling pathway did not develop a significant increase in TIF during this time (Fig. 7 *A* and *B*) despite efficient telomerase inhibition (Fig. S7 *C* and *D*). In addition, the sensitivity of cancer cells with deregulated MAP kinase signaling pathways to telomerase inhibition could be increased significantly by additionally elevating the levels of DNA replication stress using hydroxyurea (Fig. 7*C*). Our data suggest that cancer cells with deregulated MAP kinase signaling pathways are particularly sensitive to telomerase inhibition, especially when combined with drug treatment that causes DNA replication stress.

Regions Resembling Senescence-Escape Are Detected in Early Stage Skin and Breast Cancers. The great majority of human cancers acquire changes that result in reactivation of telomerase expression. Because telomerase-positive cancers, including melanoma and ductal breast carcinomas, can develop from precursor lesions that comprise senescent cells, it is possible that reactivation of telomerase in these senescent cells can also destabilize OIS in human cancer precursor lesions, thereby promoting cancer progression. Immunostaining human skin and breast tissues at various stages during cancer development using antibodies against and HP1β, a heterochromatin protein whose abundance increases as cells undergo senescence (31), as well as antibodies against hTERT revealed a protein expression pattern that is consistent with this hypothesis. In ductal breast hyperplasias and dysplastic nevi, benign neoplastic lesions that comprise cells with features of TDIS (1), abundance of hTERT protein was generally low, whereas HP1β levels were high (Fig. 8). Regions in which cells displayed high hTERT expression levels could be detected in intermediate stages of cancer development, such as ductal carcinoma in situ and melanoma in situ. In these lesions, cells with high levels of hTERT also displayed high levels of HP1β, which is in line with the model that telomerase-positive cells emerged from cells that were previously senescent (Fig. 8). High levels of hTERT and HP1β were also detected in ductal carcinomas and melanomas, but not in normal tissue, suggesting that these cancers also developed from cells that may have initially been senescent (Fig. 8 and Fig. S8). Interestingly, we did not detect any cells that displayed high hTERT and low HP1β levels in analyzed lesions. Our data are consistent with the model that derepression of *hTERT* expression also promotes escape from cellular senescence during cancer progression in humans.

Discussion

In this study, we demonstrate that cells can escape OIS after they had remained in a seemingly stable senescence arrest for long periods. To escape OIS, cells had to overcome the barriers that suppress telomerase expression, including epigenetic silencing of the *hTERT* promoter and a tight regulation of transcription factors that promote *hTERT* gene expression (23, 24). We show that cells that had remained in H-Ras^{G12V}– and B-Raf^{V600E}–induced senescence for at least 1 mo acquired changes that allowed them to break these two barriers. Although derepression of the *hTERT* promoter was facilitated by oncogene-induced chromatin reorganization, an ERK/MAP kinase-dependent stabilization and expression of c-Myc promoted transcriptional activation necessary to synthesize the rate-limiting component of telomerase, hTERT. Consistent with our previous data (1), high hTERT expression levels and telomerase activity consequently destabilized an otherwise robust proliferative arrest caused by overexpression of H-Ras^{G12V} and B-Raf^{V600E}.

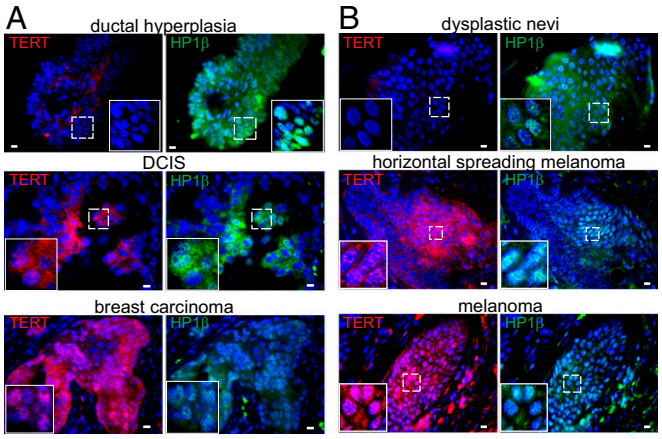

Fig. 8. Telomerase-positive cells that retain high levels of HP1b are detected in precursor lesions to melanoma and breast carcinomas. (*A*) Tissue sections from ductal hyperplasia (DH) of the breast, ductal carcinoma in situ (DCIS), and invasive breast carcinomas were immunostained with antibodies against hTERT (red; *Left*) and HP1β (green; *Right*). (*B*) Tissue sections from dysplastic nevi, horizontal spreading melanoma, and melanoma in deep soft tissue were immunostained with antibodies against hTERT (red; *Left*) and HP1β (green; *Right*). (*A, Insets*, and *B, Insets*) Enlarged version of areas indicated with dashed lines. (Scale bars: 10 μm.) A minimum of three patient samples was analyzed for each cancer grade.

Since first described almost two decades ago, cellular senescence induced by oncogenic H-Ras, as well as by downstream mediators and effectors, has been evaluated in numerous studies that collectively have contributed to uncovering the mechanistic details of this tumor-suppressing mechanism (5). Because most studies did not report on the long-term stability of H-Ras^{G12V}– and B-Raf^{V600E}–induced cellular senescence, it remained unclear whether cells actually arrested irreversibly or, alternatively, whether they entered a state of quasi-senescence from which they eventually could escape. Although our data provide strong evidence that epigenetic changes facilitate a true escape from H-Ras^{G12V}– and B-Raf^{V600E}–induced cellular senescence, we cannot rule out the possibility that some or all of the oncogene-expressing cells never underwent a stable senescence arrest before reentering the cell-division cycle. Furthermore, it is unclear whether senescence induced by these or other oncogenes is inherently less stable compared with, for example, replicative senescence in which cells can remain stably arrested for at least 3 y (32). Therefore, a deeper understanding of what characterizes a fully executed senescence program is needed, not only to better define different states of cellular senescence, but also to develop senescence lineage tracer models that can reliably track cells that had escaped OIS.

c-Myc transactivates *hTERT* expression by binding to E-boxes in the promoter region of the *hTERT* gene (33, 34). Because of a repressive chromatin state at the *hTERT* promoter and low abundance of the c-Myc protein, however, levels of hTERT are generally very low in somatic human cells. Significantly, signaling through the Ras/B-Raf MAP kinase pathway increases c-Myc protein levels, not only by suppressing its degradation (35, 36), but also by promoting *c-Myc* gene expression (37). Surprisingly, yet consistent with our data, c-Myc mRNA levels remain elevated in human cells that had undergone H-Ras^{G12V}–induced senescence, despite their exit from the cell-division cycle (38). Cells that had undergone H-Ras^{G12V}– and B-Raf^{V600E}–induced senescence therefore continuously synthesize a transcription factor capable of promoting *hTERT* gene expression.

Chromatin changes associated with cellular senescence are thought to repress expression of growth-promoting genes, while derepressing genes required for senescence induction, maintenance, and cell survival (39). Significantly, our data demonstrate that these changes eventually also cause derepression of *hTERT*, as evidenced by increased *hTERT* gene expression and increased telomerase activity, a switch from repressive to active chromatin marks at the *hTERT* promoter, and the exclusion of sites of *hTERT* transcription from SAHF. These changes may be specific for oncogene-expressing cells, because derepression of *hTERT* transcription is not observed in cells that had undergone replicative senescence, even for prolonged periods (40). Furthermore, derepression of *hTERT* transcription is a process that develops over time, because hTERT transcripts, protein, and activity can be detected at the earliest only after ∼1 mo in OIS. Supporting this interpretation are data demonstrating absence of increased hTERT expression at time points earlier than 30 d (38), which is consistent with our data. Our results therefore suggest that the chromatin landscape in cells that had undergone OIS is constantly changing, thereby placing these cells at risk for escaping an otherwise stable proliferative arrest. In senescent cells that are primed for *hTERT* expression because of continuous expression and stabilization of c-Myc, including those that express H-Ras^{G12V} and B-Raf^{V600E}, such chromatin changes would ultimately result in reactivation of telomerase activity.

In addition to its ability to suppress telomere erosion by extending short telomeres, telomerase can synthesize new telomeric sequences at DSBs by a process termed chromosome healing (41). Given that chromosome healing occurs at much greater frequencies at DSBs generated in subtelomeric regions compared with interstitial regions, it is likely that this activity of telomerase evolved as a mechanism to facilitate repair of DNA lesions in telomeric repeats. A critical question that remains unanswered, however, is whether telomeric DSBs, or dysfunctional telomeres, can be repaired by telomerase, even after they have activated a persistent DDR. If telomerase indeed could repair dysfunctional telomeres, cells that had undergone senescence due to telomere dysfunction—such as those comprising a number of distinct human cancer precursor lesions including melanocytic nevi, ductal hyperplasias of the breast, and colonic adenomas (1)—would retain the potential to continue proliferating after years in senescence, thereby posing a risk to affected patients. Our data demonstrate that reactivation of telomerase expression can significantly reduce the abundance of telomeric DDR foci in human cells after they had been generated, suggesting that telomerase can indeed repair dysfunctional telomeres. Recent studies that demonstrate a requirement for DNA damage checkpoint kinases ATM and ATR for extending telomeric repeats after DSB formation and DNA replication fork stalling, respectively, support our conclusions that telomerase is also recruited to telomeric lesions after DNA damage checkpoint kinases become activated (42, 43).

Recently discovered *hTERT* promoter mutations have been shown to promote telomerase expression by creating additional consensus binding sites for ETS family transcription factors and by triggering an epigenetic switch from inactive to active chromatin at the *hTERT* promoter (25, 26, 44). Most cancers, however, reactivate telomerase expression by mechanisms that are independent of promoter mutations. Our data provide an additional mechanism for transcriptional activation of *hTERT* during cancer progression in humans—one that may be independent of promoter mutations and that requires cells to first undergo chromatin changes associated with OIS. In line with this interpretation are our observations that hTERT-positive cells in intermediate- and late-stage human breast and melanocytic skin cancers also display high levels of HP1β, a heterochromatin protein whose abundance peaks in senescent cells (31). Because we did not detect any cells that simultaneously displayed high levels of hTERT and low levels of HP1β, our data suggest that cancer cells emerged from HP1β-positive and therefore senescent somatic cells in analyzed lesions. This interpretation is

consistent with linear melanoma and breast cancer progression models and is supported by clinical observations that certain premalignant breast and melanocytic skin lesions, which are composed of senescent cells (1), can reside nonrandomly and in close proximity to their malignant cancer counterparts (45–49).

Our data demonstrating that cells can eventually escape cellular senescence due to oncogene-induced derepression of *hTERT* expression have important clinical implications. Deregulation of the Ras–MAP kinase pathway, either because of aberrant activation of upstream receptor-mediated signaling cascades or as a consequence of mutations directly in Ras and downstream effector kinases, is observed in most human cancers (50). If these are driver mutations that cause cells to first hyperproliferate and then undergo a senescence response that is stabilized due to the formation of dysfunctional telomeres—similar to what is observed in melanocytic nevi, ductal breast hyperplasias, and colonic adenomas (1)—patients affected by such cancer precursor lesions may be at risk for developing more advanced-stage cancers because of the potential of telomerase reactivation and senescence escape. However, because these cells may still retain DDRs, they are still targetable using DNA-damaging agents, as we demonstrate in this study. In addition, because Ras–MAP kinase signaling is essential for *hTERT* expression in cells that had escaped OIS, conventional inhibitors of this signaling pathway may even be effective in inhibiting telomerase activity in early transformed human cancer cells, as our data would suggest (51).

Materials and Methods

Cell Culture and Reagents. Human diploid dermal fibroblasts (HSF43), BJ (ATCC), and GM21808 (Coriell) were cultured in Ham's F-10 medium (Life Technologies) supplemented with 15% (vol/vol) batch-tested FBS (Atlanta Biologicals). Human breast cancer cell lines (MDA-MB-231 and -468), a colon cancer cell line (HCT116), and a fibrosarcoma cell line (HT-1080) were grown in Dulbecco's modified Eagle medium (Life Technologies) supplemented with 10% (vol/vol) FBS (Atlanta Biologicals). All cell lines were maintained at 37 °C in an atmosphere of 5% CO_2. Growth curves were generated by using a hemocytometer and the formula PD = $\log2(N_{final}/N_{initial})$, where $N_{initial}$ is the number of cells seeded at each passage and N_{final} is the number of cells recovered from the dish. To measure cellular senescence, proliferating cells were labeled with 10 μM EdU for 24 h, and EdU-positive cells were detected by using the ClickiT EdU Alexa Fluor 488 imaging kit (Invitrogen) according to manufacturer's instructions. Drugs Zeocin (Life Technologies), hydroxyurea (Sigma-Aldrich), and aphidicolin (Sigma-Aldrich) were directly added to the culture medium. MEK1/2 inhibitor U0126 was obtained from Sigma-Aldrich.

Cell Viability Assay. Cells were seeded at equal density, and after drug treatment, cell numbers and percentage viability were measured by automatic cell counting using the Vi-CELL XR cell counter (Beckman Coulter). The cell counter discriminates dead and viable cells using the trypan blue method.

Plasmid and Transduction. pBABE-Puro H-Ras^{G12V} (Addgene plasmid 1768), pBABE-puro- B-Raf^{V600E} (Addgene plasmid 17544), pBabe-puro (Addgene plasmid 1764), CDC6, pLenti-sh1368 knockdown c-Myc (Addgene plasmid 29435), pBabe-puro hTERT (Addgene plasmid 1771), pBabe-puro-DNhTERT (Addgene plasmid 1775), pMKO.1 puro hTERT shRNA (Addgene plasmid 10688), and pMKO.1 puro GFP shRNA (Addgene plasmid 10675) were used. By using the calcium phosphate precipitation method, retroviral particles were produced by transfecting the packaging cell lines, Platinum-A (Cell Biolabs) with the vector of interest. After transfection, viral supernatants were collected, and target cells were transduced with virus. Cells were selected with 1 μg/mL puromycin (Sigma-Aldrich) for 48 h.

Immunoblotting. Protein extracts were prepared in radioimmunoprecipitation assay lysis buffer (Thermo Scientific) containing 500 μM PMSF and 1:100 protease inhibitor mixture. A total of 20 μg of whole cell lysates were resolved on SDS/PAGE (8% or 12%), and proteins were transferred to PVDF membranes (Pall Life Sciences) and probed as described (1). The following primary antibodies were used: ATM-s1981, p21 (C-19; Santa Cruz); anti–p53-S15 (Cell Signaling Technology); γH2AX(S139) (Upstate); anti-Ras (BD Transduction Laboratories); Cdc6 (180.2) sc-9964 and Raf-B (F-7) sc-5284 (Santa Cruz); and γ-tubulin (Sigma-Aldrich), and HRP-conjugated goat anti-rabbit (PerkinElmer) or mouse antibodies (Cell Signaling) were used as secondary antibodies.

RNA-FISH. Cultured cells were fixed with 4% (wt/vol) paraformaldehyde (PFA) for 10 min, permeabilized with 70% (vol/vol) ethanol for 1 h followed by overnight hybridization with 20 μL of TERT-RNA FISH probe (Stellaris no. VSMF-2410-5) at 37 °C. Coverslips were subsequently incubated with wash buffer A (Stellaris no. SMF-WA1-60) containing DAPI (5 ng/mL) for 30 min followed by a 5-min wash with wash buffer B (Stellaris no. SMF-WB1-20) and mounted with Vectashield mounting medium (Vector Laboratories).

Immuno-FISH. To detect TIF, cells were fixed, permeabilized, and blocked as above and subsequently serially dehydrated by placing them in 70%, 80%, and 95% (vol/vol) ethanol for 3 min each. After air-drying, nuclear DNA was denatured for 5 min at 80 °C in hybridization buffer containing Cy3-conjugated telomere-specific PNA [Cy3-$(C_3TA_2)_3$; Panagene] at a concentration of 0.5 μg/mL, 70% (vol/vol) formamide, 12 mM Tris·HCl (pH 8.0), 5 mM KCl, 1 mM $MgCl_2$, 0.08% Triton X-100, and 0.25% acetylated BSA (Sigma-Aldrich), followed by incubation in the same buffer overnight at room temperature. Coverslips were washed sequentially with 70% (vol/vol) formamide/0.6× SSC [90 mM NaCl, 9 mM Na–citrate (pH 7); three times for 15 min each], 2× SSC (15 min), and [PBS + 0.1% Tween 20 (PBST); 5 min] followed by immunostaining for DSBs by using the indicated primary antibodies (53BP1 or γH2AX) and secondary Alexa Fluor 488-conjugated goat anti-rabbit antibodies (Invitrogen).

Telomere Length Measurements Using qFISH. Relative telomere lengths were assessed by quantification of telomeric signal fluorescence intensities of cells processed by immuno-FISH using the ImageJ software (Version 1.45) and the object counter 3D plugin on images acquired by using a Zeiss Axiovision 200M microscope equipped with ApoTome as described (1, 10).

Immunostaining Cells and Tissue. Cultured cells were fixed with 4% (wt/vol) PFA, permeabilized with PBS containing 0.2% Triton X-100 for 20 min each, and blocked with 4% (wt/vol) BSA in PBST for 30 min. Primary antibodies anti-53BP1 (Novus; 1:1,000), anti-γH2AX(S139) (Upstate; 1:1,000), anti-TERT (Abcam; 1:500), or anti-HP1β (EMD Millipore; 1:50) were incubated for 2 h at room temperature or overnight at 4 °C in block buffer. After three 10-min washes with PBST, cells were incubated with secondary antibodies as indicated for 1 h at room temperature. Slides were washed three times for 10 min with PBST, air-dried, and mounted by using DAPI-containing mounting medium (Vector Laboratories).

Archival and paraffin embedded tumor tissue was obtained from the tumor tissue bank at New Jersey Medical School with the approval of the local institutional review board committee. Four-μm tissue sections were deparaffinized and incubated in sodium citrate buffer (10 mM Na–citrate, 0.05% Tween 20, pH 6) at 95 °C for 45 min to retrieve antigens. Tissue sections were subsequently rinsed with water and incubated overnight with block buffer (4% BSA in PBST). Tissue sections were incubated with primary antibodies Tert and HP1β for 2 h at 37 °C in block buffer. After three 10-min washes with PBST, tissue sections were incubated with secondary antibodies as indicated (1:1,000 in block buffer) for 1 h at 37 °C. Slides were washed three times for 10 min with PBST, rinsed with water, and mounted by using DAPI-containing mounting medium (Vector Laboratories).

Microscopy. Images were acquired using a Zeiss Axiovert 200M microscope, an AxioCamMRm camera (Zeiss), and AxioVision software (Version 4.6.3; Zeiss). To analyze and quantitate colocalization between telomere signals and DSB foci, images were acquired as *z*-series (three to five images, 0.5-μm optical slices) using a motorized stage, a 63×/1.4 oil immersion lens, and an ApoTome (Zeiss). ApoTome microscopy eliminates out-of-focus light and generates shallow focal planes (0.5 μM using a 63× oil objective). To quantitate DDR foci, random images were acquired by using a 63×/1.4 oil immersion lens.

Generation and Expression of Dox-Controlled hTERT (iTERT). iTERT was generated by using Retro-XTM Tet-On 3G inducible expression system (catalog no. 631188; Clontech). hTERT cDNA was excised from pBabe-puro hTERT and subcloned into the multiple cloning site of pRetroX TRE 3G vector. Retroviruses were generated according to manufacturer's protocol. GM21 human dermal fibroblasts were transduced simultaneously with pRetroX TRE 3G hTERT and pRetroX Tet 3G retroviruses twice per day and repeated for 3 d. Cells were selected with neomycin and puromycin. The cells were maintained either in the presence or absence of indicated amounts of dox.

Telomerase Activity. Telomerase activity was measured by the TRAPeze RT Telomerase detection Kit (EMD Millipore), using PCR and Amplifluor primers according to the manufacturer's instructions. Pelleted cells were resuspended in CHAPS lysis buffer, incubated on ice for 30 min, and spun to collect the supernatant. A total of 250 ng of protein lysates was used to detect telomerase activity using the Real-Time PCR system (Bio-Rad).

Quantitative values of the telomerase activity were obtained from a standard curve generated by using dilutions of control template provided by the kit.

Real-Time qPCR. Total RNA was isolated from cells by using RNeasy (Qiagen) according to the manufacturer's instructions and treated with RNase-free DNase (Qiagen) before reverse transcription. Then, 1 μg of total RNA was reverse-transcribed by using the iScriptTM cDNA synthesis kit (Bio-Rad). qPCR was performed by using specific primers with the iTaq Universal SYBR green supermix (Bio-Rad) on a CFX96 Touch Real-Time PCR detection system (Bio-Rad). Samples were analyzed in duplicates, and GAPDH levels were used for normalization. Primer sequences for RT-qPCR were as follows: c-Myc: forward primer, 5′-ACCACCAGCAGCGACTCTGA-3′, and reverse primer, 5′-TCCAGCAGAAGGTGATCCAGACT-3′; hTERT: forward primer, 5′-CGGAAGAGTGTCTGGAGCAA-3′, and reverse primer, 5′-TGACCTCCGTGAGCCTGTC-3′; Ras: forward primer, 5′-CCAGCTGATCCAGAACCATT-3′, and reverse primer, 5′-GGTATCCAGGATGTCCAACAG-3′; and GAPDH: forward primer, 5′-CTCTCTGCTCCTCCTGTTCGAC-3′, and reverse primer, 5′-TGAGCGATGTGGCTCGGCT-3′.

Colony Formation Assay. Approximately 5,000 cells were mixed with a final concentration of 0.3% agar and F-10 medium containing 10% FBS and plated in triplicates onto six-well dishes containing a basal layer of 0.8% agar containing F-10 medium and 10% FBS. The plates were kept in a humidified incubator at 37 °C with 5% CO_2 for 3 wk, and fresh medium was added every 4 d. After 3 wk, digital images of 10 random fields were acquired by using a microscope (EVOS), and colonies were counted manually.

qChIP Assay. The ChIP assay was carried out according to the protocol from EMD Millipore. Cells were cross-linked by incubating them in 1% (vol/vol) formaldehyde containing medium for 10 min at 37 °C and then sonicated six times for 5 s each to obtain DNA fragments of 200–1,000 bp in length. Antibodies against Acetyl H4 (EMD Millipore catalog no. 06-866), H3K9Me3 (EMD Millipore catalog no. 07-442), H3K9Ac (EMD Millipore catalog no. 07-352), H3K4Me3 (EMD Millipore catalog no. 07-473), or c-Myc (Santa Cruz catalog no. sc-40x) were used to precipitate DNA fragments, and the protein–DNA complex was collected with protein-G Sepharose beads, eluted, and reverse cross-linked. Extracted samples were then purified by using spin columns, and recovered DNA was used for qPCR. Primer sequences for the hTERT promoter were 5′-CCA GGC CGG GCT CCC AGT GGA T-3′ (forward) and 5′-GGC TTC CCA CGT GCG CAG CAG GA-3′ (reverse). Primers for GAPDH were 5′-AAA GGG CCC TGA CAA CTC TT-3′ (forward) and 5′-GGT GGT CCA GGG GTC TTA CT-3′ (reverse). Primers for the hTERT distal promoter were 5′-GCT TGC AGA GGT GGC TCT-3′ (forward) and 5′-GCT GTG GTT TGG GAG ACT AAA-3′ (reverse).

ACKNOWLEDGMENTS. U.H. was supported by NIH National Cancer Institute Grants R01CA136533 and R01CA184572. O.B. was supported by grants from ANR-BMFT, Foundation ARC pour la recherche sur le Cancer, and Association La Ligue National Contre le Cancer LNCC. O.B. is a CNRS fellow.

1. Suram A, et al. (2012) Oncogene-induced telomere dysfunction enforces cellular senescence in human cancer precursor lesions. *EMBO J* 31(13):2839–2851.
2. Collado M, Serrano M (2010) Senescence in tumours: Evidence from mice and humans. *Nat Rev Cancer* 10(1):51–57.
3. Kuilman T, Michaloglou C, Mooi WJ, Peeper DS (2010) The essence of senescence. *Genes Dev* 24(22):2463–2479.
4. Muñoz-Espín D, Serrano M (2014) Cellular senescence: from physiology to pathology. *Nat Rev Mol Cell Biol* 15(7):482–496.
5. Serrano M, Lin AW, McCurrach ME, Beach D, Lowe SW (1997) Oncogenic *ras* provokes premature cell senescence associated with accumulation of p53 and $p16^{INK4a}$. *Cell* 88(5):593–602.
6. Michaloglou C, et al. (2005) $BRAF^{E600}$-associated senescence-like cell cycle arrest of human naevi. *Nature* 436(7051):720–724.
7. Sears RC, Nevins JR (2002) Signaling networks that link cell proliferation and cell fate. *J Biol Chem* 277(14):11617–11620.
8. Di Micco R, et al. (2006) Oncogene-induced senescence is a DNA damage response triggered by DNA hyper-replication. *Nature* 444(7119):638–642.
9. Bartkova J, et al. (2006) Oncogene-induced senescence is part of the tumorigenesis barrier imposed by DNA damage checkpoints. *Nature* 444(7119):633–637.
10. Fumagalli M, et al. (2012) Telomeric DNA damage is irreparable and causes persistent DNA-damage-response activation. *Nat Cell Biol* 14(4):355–365.
11. Hewitt G, et al. (2012) Telomeres are favoured targets of a persistent DNA damage response in ageing and stress-induced senescence. *Nat Commun* 3:708.
12. Funayama R, Saito M, Tanobe H, Ishikawa F (2006) Loss of linker histone H1 in cellular senescence. *J Cell Biol* 175(6):869–880.
13. Zhang R, Chen W, Adams PD (2007) Molecular dissection of formation of senescence-associated heterochromatin foci. *Mol Cell Biol* 27(6):2343–2358.
14. Di Micco R, et al. (2011) Interplay between oncogene-induced DNA damage response and heterochromatin in senescence and cancer. *Nat Cell Biol* 13(3):292–302.
15. Narita M, et al. (2003) Rb-mediated heterochromatin formation and silencing of E2F target genes during cellular senescence. *Cell* 113(6):703–716.
16. Herbig U, Jobling WA, Chen BP, Chen DJ, Sedivy JM (2004) Telomere shortening triggers senescence of human cells through a pathway involving ATM, p53, and p21(CIP1), but not p16(INK4a). *Mol Cell* 14(4):501–513.
17. d'Adda di Fagagna F, et al. (2003) A DNA damage checkpoint response in telomere-initiated senescence. *Nature* 426(6963):194–198.
18. Sfeir A, et al. (2009) Mammalian telomeres resemble fragile sites and require TRF1 for efficient replication. *Cell* 138(1):90–103.
19. Martínez P, et al. (2009) Increased telomere fragility and fusions resulting from TRF1 deficiency lead to degenerative pathologies and increased cancer in mice. *Genes Dev* 23(17):2060–2075.
20. Suram A, Herbig U (2014) The replicometer is broken: Telomeres activate cellular senescence in response to genotoxic stresses. *Aging Cell* 13(5):780–786.
21. Artandi SE, DePinho RA (2010) Telomeres and telomerase in cancer. *Carcinogenesis* 31(1):9–18.
22. Atkinson SP, Hoare SF, Glasspool RM, Keith WN (2005) Lack of telomerase gene expression in alternative lengthening of telomere cells is associated with chromatin remodeling of the hTR and hTERT gene promoters. *Cancer Res* 65(17):7585–7590.
23. Zhu J, Zhao Y, Wang S (2010) Chromatin and epigenetic regulation of the telomerase reverse transcriptase gene. *Protein Cell* 1(1):22–32.
24. Daniel M, Peek GW, Tollefsbol TO (2012) Regulation of the human catalytic subunit of telomerase (hTERT). *Gene* 498(2):135–146.
25. Stern JL, Theodorescu D, Vogelstein B, Papadopoulos N, Cech TR (2015) Mutation of the TERT promoter, switch to active chromatin, and monoallelic TERT expression in multiple cancers. *Genes Dev* 29(21):2219–2224.
26. Heidenreich B, Rachakonda PS, Hemminki K, Kumar R (2014) TERT promoter mutations in cancer development. *Curr Opin Genet Dev* 24:30–37.
27. Hahn WC, et al. (1999) Inhibition of telomerase limits the growth of human cancer cells. *Nat Med* 5(10):1164–1170.
28. Masutomi K, et al. (2003) Telomerase maintains telomere structure in normal human cells. *Cell* 114(2):241–253.
29. Wojtyla A, Gladych M, Rubis B (2011) Human telomerase activity regulation. *Mol Biol Rep* 38(5):3339–3349.
30. Kyo S, Takakura M, Fujiwara T, Inoue M (2008) Understanding and exploiting hTERT promoter regulation for diagnosis and treatment of human cancers. *Cancer Sci* 99(8):1528–1538.
31. Kreiling JA, et al. (2011) Age-associated increase in heterochromatic marks in murine and primate tissues. *Aging Cell* 10(2):292–304.
32. Fumagalli M, Rossiello F, Mondello C, d'Adda di Fagagna F (2014) Stable cellular senescence is associated with persistent DDR activation. *PLoS One* 9(10):e110969.
33. Wang J, Xie LY, Allan S, Beach D, Hannon GJ (1998) Myc activates telomerase. *Genes Dev* 12(12):1769–1774.
34. Wu KJ, et al. (1999) Direct activation of TERT transcription by c-MYC. *Nat Genet* 21(2):220–224.
35. Sears R, Leone G, DeGregori J, Nevins JR (1999) Ras enhances Myc protein stability. *Mol Cell* 3(2):169–179.
36. Sears R, et al. (2000) Multiple Ras-dependent phosphorylation pathways regulate Myc protein stability. *Genes Dev* 14(19):2501–2514.
37. Kerkhoff E, et al. (1998) Regulation of c-myc expression by Ras/Raf signalling. *Oncogene* 16(2):211–216.
38. Nelson DM, McBryan T, Jeyapalan JC, Sedivy JM, Adams PD (2014) A comparison of oncogene-induced senescence and replicative senescence: implications for tumor suppression and aging. *Age (Dordr)* 36(3):9637.
39. Corpet A, Stucki M (2014) Chromatin maintenance and dynamics in senescence: A spotlight on SAHF formation and the epigenome of senescent cells. *Chromosoma* 123(5):423–436.
40. De Cecco M, et al. (2013) Genomes of replicatively senescent cells undergo global epigenetic changes leading to gene silencing and activation of transposable elements. *Aging Cell* 12(2):247–256.
41. Ribeyre C, Shore D (2013) Regulation of telomere addition at DNA double-strand breaks. *Chromosoma* 122(3):159–173.
42. Lee SS, Bohrson C, Pike AM, Wheelan SJ, Greider CW (2015) ATM kinase is required for telomere elongation in mouse and human cells. *Cell Reports* 13(8):1623–1632.
43. Tong AS, et al. (2015) ATM and ATR signaling regulate the recruitment of human telomerase to telomeres. *Cell Reports* 13(8):1633–1646.
44. Bell RJ, et al. (2015) Cancer. The transcription factor GABP selectively binds and activates the mutant TERT promoter in cancer. *Science* 348(6238):1036–1039.
45. Smolle J, Kaddu S, Kerl H (1999) Non-random spatial association of melanoma and naevi—a morphometric analysis. *Melanoma Res* 9(4):407–412.
46. Allred DC, et al. (2008) Ductal carcinoma in situ and the emergence of diversity during breast cancer evolution. *Clin Cancer Res* 14(2):370–378.
47. Allred DC, Mohsin SK, Fuqua SA (2001) Histological and biological evolution of human premalignant breast disease. *Endocr Relat Cancer* 8(1):47–61.
48. Miller AJ, Mihm MC, Jr (2006) Melanoma. *N Engl J Med* 355(1):51–65.
49. Vredeveld LC, et al. (2012) Abrogation of BRAFV600E-induced senescence by PI3K pathway activation contributes to melanomagenesis. *Genes Dev* 26(10):1055–1069.
50. Dhillon AS, Hagan S, Rath O, Kolch W (2007) MAP kinase signalling pathways in cancer. *Oncogene* 26(22):3279–3290.
51. Samatar AA, Poulikakos PI (2014) Targeting RAS-ERK signalling in cancer: Promises and challenges. *Nat Rev Drug Discov* 13(12):928–942.